

## Statistical and biological uncertainties associated with vaccine efficacy estimates and their implications for dengue vaccine impact projections

T. Alex Perkins<sup>1,2\*</sup>, Robert C. Reiner<sup>2,3</sup>, Quirine A. ten Bosch<sup>1</sup>, Guido España<sup>1</sup>, Amit Verma<sup>4</sup>, Kelly A. Liebman<sup>5</sup>, Valerie A. Paz-Soldan<sup>6</sup>, John P. Elder<sup>7</sup>, Amy C. Morrison<sup>5</sup>, Steven T. Stoddard<sup>7</sup>, Uriel Kitron<sup>2,8</sup>, Gonzalo M. Vazquez-Prokopec<sup>2,8</sup>, Thomas W. Scott<sup>2,5</sup>, David L. Smith<sup>2,3</sup>

<sup>1</sup> Department of Biological Sciences and Eck Institute for Global Health, University of Notre Dame, Notre Dame, IN

<sup>2</sup> Fogarty International Center, National Institutes of Health, Bethesda, MD

<sup>3</sup> Institute for Health Metrics and Evaluation, University of Washington, Seattle, WA

<sup>4</sup> Center for Disease Dynamics, Economics, and Policy, Washington, DC

<sup>5</sup> Department of Entomology and Nematology, University of California, Davis, CA

<sup>6</sup> Department of Global Community Health and Behavioral Sciences, Tulane University School of Public Health and Tropical Medicine, New Orleans, LA

<sup>7</sup> Institute for Behavioral and Community Health, Graduate School of Public Health, San Diego State University, San Diego, CA

<sup>8</sup> Department of Environmental Sciences, Emory University, Atlanta, GA

\* Author for correspondence: [taperkins@nd.edu](mailto:taperkins@nd.edu)

### ABSTRACT

Given the limited effectiveness of strategies based solely on vector control to reduce dengue virus transmission, it is expected that an effective vaccine could play a pivotal role in reducing the global disease burden of dengue. Dengvaxia® from Sanofi Pasteur recently became the first dengue vaccine to become licensed in select countries and to achieve WHO recommendation for use in certain settings, despite the fact that a number of uncertainties about the vaccine's efficacy and mode of action complicate projections of its potential impact on public health. We used a new stochastic individual-based model for dengue transmission to perform simulations of the impact of Dengvaxia® in light of two key uncertainties: statistical uncertainty about the numerical value of the vaccine's efficacy against disease, and biological uncertainty about the extent to which its efficacy against disease derives from the amelioration of symptoms, blocking of dengue infection, or some combination thereof. Our results suggest that projections of the vaccine's public health impact may be far more sensitive to biological details of how the vaccine protects against disease than to statistical details of the extent to which it protects against disease. Under the full range of biological uncertainty that we considered, there was nearly three-fold variation in the population-wide number of disease episodes averted. These differences owe to variation in indirect effects of vaccination arising from uncertainty about the extent of onward transmission of dengue from vaccine recipients. These results demonstrate important limitations associated with the use of symptomatic disease as the primary endpoint of dengue vaccine trials and highlight the importance of considering multiple forms of uncertainty in projections of a vaccine's impact on public health.

## INTRODUCTION

Dengue is one of the most significant mosquito-borne viral diseases on the planet, having reemerged in the last few decades as a major burden on global health (1). To date, the control and prevention of dengue has relied exclusively on various forms of vector control (2), which have experienced success in certain cases but have not been sufficient to prevent the reemergence of this disease on a global scale (3). At the same time, several vaccine candidates for dengue have been under development for a number of years (4), with the Dengvaxia® vaccine from Sanofi Pasteur recently becoming licensed in some countries and recommended for use under certain circumstances by the World Health Organization (5).

A number of concerns about Dengvaxia® arose during clinical trials, the results of which indicated relatively low efficacy overall (6). In particular, efficacy against disease was significantly lower for children under 9 years of age (44%) compared with children 9 years of age or older (65%). The vaccine also appeared to provide higher protection to seropositive than to seronegative recipients, especially at young ages (2-5 years). Estimates of vaccine efficacy appeared to vary among the four serotypes, with lower efficacy reported for serotype 2 (6). We refer to these collective uncertainties about the numerical value of vaccine efficacy as “statistical uncertainty.”

Another major source of uncertainty associated with the Dengvaxia® vaccine has to do with the clinical nature of the trial endpoints. Specifically, the primary endpoint for all clinical trials was virologically confirmed dengue among trial participants who experienced acute febrile illness: i.e., a fever of  $\geq 38$  °C for at least two consecutive days (6). This choice of endpoint is potentially problematic, because a large proportion of dengue infections result in either mild symptoms or no detectable symptoms whatsoever (7) yet are nonetheless capable of infecting mosquitoes (8). Thus, it is completely unclear whether Dengvaxia® confers any form of protection to individuals who would not have experienced acute febrile illness in the first place. Among those for whom acute febrile illness was averted due to vaccination, it is unclear whether the vaccine blocked dengue virus infection altogether or ameliorated symptoms but still allowed for infection and onward transmission. We refer to this combination of unknown factors as “biological uncertainty.”

In addition to fundamental challenges that biological uncertainty poses for the estimation of vaccine efficacy from trial data (9), its implications for projections of vaccine public health impact are also potentially quite substantial. In the event that the vaccine achieves its clinically observed efficacy by ameliorating symptoms but has no impact on infection and onward transmission, its public health impact would be readily predictable: vaccine recipients would experience *direct* effects in the form of reduced incidence of disease and everyone else would experience the same incidence of disease as they would have in the absence of the vaccine. To the extent that the vaccine blocks infection, it is possible that the vaccine could also confer *indirect* effects at a population level by preventing onward transmission from vaccine recipients.

To assess the relative impact on public health of vaccines that differ in these ways, we simulated dengue transmission in the presence and absence of routine vaccination with vaccines representing a wide range of joint statistical and biological uncertainty. We performed these simulations with a new individual-based simulation model of dengue transmission that we developed for the city of Iquitos, Peru, which has had ongoing studies of dengue epidemiology for nearly two decades (10,11). One advantage of our new model relative to existing simulation models of dengue transmission (12,13) is that it features the most realistic model available for fine-scale human movement in a dengue-endemic area (14), which is an essential feature for realistic quantification of the potential indirect effects of vaccination.

## METHODS

### Model overview

We developed a stochastic, individual-based model for simulating dengue transmission that is parameterized in a number of respects around studies of dengue epidemiology conducted in Iquitos, Peru. The model simulates dengue transmission in a population of approximately 200,000 people residing in the core of the city of Iquitos, which consists of 38,835 geo-referenced houses and 2,004 other buildings (15). Events such as mosquito biting, mosquito death, and movements by humans and mosquitoes are scheduled to occur at continuous time points throughout the day (Fig. 1), with updating of individuals' statuses with respect to infection, immunity, and in other respects occurring once daily. We described the model in full detail in the Supporting Information, following the ODD (Overview, Design concepts, Details) Protocol (16,17) for describing individual-based models. In the three paragraphs below, we highlight key features of the model pertaining to humans, mosquitoes, and viruses, respectively.

Humans are populated in the city consistent with national age and gender distributions for Peru and in individual houses consistent with demographic data collected over the course of studies in Iquitos. Birth and death processes are parameterized so as to result in a demographically stable population, with individuals who die being replaced by a newborn in the same house. Aging involves the acquisition of lifelong, serotype-specific immunity as one is exposed and sex-specific growth of an individual's body size over the course of childhood. Each individual human possesses a unique "activity space," which is defined as an average pattern of time allocation across all the locations that they frequent (18). Individuals move about this activity space in a manner previously described in detail by Perkins et al. (14).

The number of adult female mosquitoes in the area is determined by two model parameters: a daily per-building emergence rate, and a daily per-capita mortality rate. Mosquitoes move from their current location to a nearby location with a fixed probability each day (19). They engage in biting at a constant rate (20) and select an individual on whom to blood feed based on who is present at a location at the time that a mosquito bites and what each person's body size is (14,21). Because the emphasis of the present analysis is on vaccination rather than vector control, we have deferred the inclusion of a number of other entomological details for future work.

The model allows for the transmission of four dengue serotypes, which are assumed to be identical in the following respects based on empirical studies: infectiousness (8,22), incubation period (23), and rate of symptomatic disease (7). Although there is evidence that vaccine efficacy differs by serotype (6), no data have been published to date that indicate how serotype-specific effects might manifest differently in individuals of different ages and serostatuses. Because serostatus-specific effects are most concerning from a safety perspective (24) and because of clear age-serostatus interactions (6), we prioritized those effects and assumed in the model that efficacy applies equally to each of the four serotypes. Viruses of each serotype are seeded into the population at a constant rate through a constant “force of importation” parameter, which is intended to mimic the introduction of the virus into the city from surrounding areas (25). Individual people can experience up to four distinct infections over the course of their lifetimes, as they experience lifelong immunity to each serotype to which they have been exposed and temporary cross immunity to all serotypes following exposure (26).

### Vaccine efficacy

The mode of action of the Dengvaxia® vaccine is unclear, given that there are multiple mechanisms by which clinical trial data could have come about (27). We modeled vaccine efficacy against disease (i.e., the primary trial endpoint) as a function of age and serostatus, which is consistent with one hypothesis for how the vaccine achieves its efficacy (6,27). Specifically, for a given serostatus, we modeled the relationship between age and vaccine efficacy against disease as

$$VE_{dis}(age) = 1 - \frac{a}{1 + \exp(b(age - c))} \quad (1)$$

using serostatus-specific values of  $a$ ,  $b$ , and  $c$ . To obtain point estimates of  $a$ ,  $b$ , and  $c$  for both seropositive and seronegative vaccine recipients, we fitted eqn. (1) under different values of these parameters to mean estimates of  $VE_{dis}$  for 2-9 and 10-16 year olds reported in Fig. 2 of Hadinegoro et al. (6) on the basis of least squares using the optim function in R (28). These calculations assumed an even age distribution within each age class in the trials.

We modeled statistical uncertainty around estimates of  $VE_{dis}$  with a parameter  $\sigma$  that describes the standard deviation of the log of the risk ratio, defined mathematically as

$$\sigma(\ln(RR_{dis})) = (1/(d + e) + 1/(d(1 - VE_{dis}) + e))^{1/2} \quad (2)$$

To fit values of  $d$  and  $e$ , we used a method based on the assumption of asymptotic normality of the log of the ratio of Poisson rates (29), applied to standard errors presented in Fig. 2 of Hadinegoro et al. (6). To then take a random draw of  $VE_{dis}$  for a given instance of the simulation with statistical uncertainty consistent with that reported by Hadinegoro et al. (6), we drew a random normal variable with mean 0 and standard deviation 1, multiplied it by  $\sigma(\ln(RR_{dis}))$ , added the result to  $\ln(1 - VE_{dis})$ , exponentiated the result, and subtracted it from 1 (6).

In a given simulation, we applied the same standard normal random draw to the calculation of  $VE_{dis}$  for all seropositive and seronegative vaccine recipients. We furthermore assumed that the vaccine is leaky, meaning that an individual has some chance of becoming infected each time they are exposed and has some chance of developing disease each time they are infected. The chances of those events happening in a vaccine recipient are lowered proportional to relative risk; specifically,  $RR_{inf|exp}$  and  $RR_{dis|inf}$ , respectively (Table 1).

## Numerical experiments

### Parameter sweep

To characterize basic relationships between free parameters in our model and epidemiological metrics of interest, we performed 1,000 simulations across different combinations of the following ranges of four unknown parameters sampled with the sobol function in the pomp package (30) in R (28): mosquito emergence rate (0.01-1.99 mosquitoes per day per building), average adult mosquito lifespan (3-10 days), infectiousness of mosquitoes to people (0.01-0.99), and “force of importation,” defined as the per capita rate at which susceptible people acquired infection from outside the simulated population ( $10^{-7}$ - $10^{-4}$ ). In each simulation in the parameter sweep, we recorded the average age of first infection (a standard metric for transmission intensity, (31)) and seroprevalence among 9 year olds (a highly relevant metric for deployment of the Dengvaxia® vaccine, (5)).

### Vaccine impact projections

To focus on uncertainties related to vaccine efficacy, we constrained uncertainties about other model parameters by adopting previously used values for infectiousness of mosquitoes to people (0.9, (32)) and daily adult female mosquito mortality rate (0.11, (33)). Because force of importation is a more difficult parameter to estimate or to extrapolate from other modeling studies, we set the value of this parameter to a value of  $5.0 \times 10^{-5}$  per person per day, which is the midpoint of the range of values that we explored in the parameter sweep. To select a value for the rate of emergence of new adult female mosquitoes, we first specified a target age-9 seroprevalence of 50% and then selected an emergence rate of 0.226 mosquitoes per location per day based on relationships between parameters and metrics identified in the parameter sweep. These choices resulted in a single set of parameters for all aspects of our model, other than properties of the vaccine.

For the parameter values specified above, we performed 2,500 pairs of simulations with random draws of  $p$  (biological uncertainty) and  $q$  (statistical uncertainty) from uniform distributions between 0 and 1 sampled across simulation pairs with the sobol function in the pomp package (30) in R (28) to maximize coverage of the  $p$ - $q$  parameter space. For each such scenario, we performed one simulation with 40 years of no vaccination and then 40 years of routine vaccination at age 9 at 90% coverage. In the other simulation in the pair, we simulated 80 years of no vaccination, the first 40 years of which were identical to the other simulation in the pair due to the fact that they shared the same random number seed. For all simulations, we recorded the

following in the population as a whole: numbers of infections averted and disease episodes averted in each year.

## RESULTS

### Parameter sweep

The four free parameters in the model were all correlated with age-9 seroprevalence and average age of first infection in the expected directions (positive and negative, respectively) (Fig. 2). In particular, the force of importation parameter in our model determined a minimum seroprevalence and maximum age of first infection. Values beyond those minima and maxima were accounted for by vectorial capacity, a composite metric of both free and fixed entomological parameters (Fig. 2). Overall, vectorial capacity and force of importation accounted for 90% and 7%, respectively, of variation in age-9 seroprevalence values (measured by  $R^2$  in a generalized additive model, (34)). Vectorial capacity and force of importation accounted for 76% and 15% of variation in age of first infection values, with an additional 6% of variation obtained by fitting a model with both variables simultaneously.

### Vaccine efficacy

We obtained best-fit estimates of the parameters for vaccine efficacy (and likewise relative risk, since  $VE = 1 - RR$ ) in eqn. (1) of  $a = 0.47$ ,  $b = 0.148$ , and  $c = 9.17$  for seropositive vaccine recipients and  $a = 1.26$ ,  $b = 0.28$ , and  $c = 9.27$  for seronegative vaccine recipients. We obtained estimates of the parameters determining the standard error of the log of the risk ratio in eqn. (2) of  $d = 100$  and  $e = 0.5$ . Under this model and with these parameters, relative risk decreased steeply with age until around age 20, when it began to decrease more slowly towards almost no risk in older people (Fig. 3). As in the clinical trial data, relative risk under our model was several fold lower in seropositive than seronegative children, and relative risk in excess of 1 was likely only at ages well below 9 years (Fig. 3).

Under our assumptions about how efficacy observed in trials derived from two separate types of protection, an assumption of equal parts protection against infection and protection against disease (i.e.,  $p = 0.5$ ) gave, on average, a relative risk of 48% for either infection or disease in seropositive 9-year olds and 80% in seronegative 9-year olds (Fig. 4). In the event that 90% of protection derived from protection against disease and only 10% from protection against infection (i.e.,  $p = 0.1$ ), then the relative risk for 9-year olds was 27% for disease and 87% for infection for seropositives and 68% for disease and 96% for infection for seronegatives (Fig. 4).

### Vaccine impact projections

In twelve randomly selected pairs of simulations (Fig. 5), dynamics in the 40 years following vaccine introduction relative to a nearly identical simulation without vaccination varied substantially. In most cases, the number and severity of epidemics was reduced. In some cases, however, epidemics occurred earlier, or more severe epidemics occurred than would have otherwise (Fig. 5). This variability was also reflected across the full collection of 2,500 pairs of simulations, with many simulations exhibiting a net increase in infections and disease for 10-20 years or more following vaccine introduction (Fig. 6A, 6B).

Although much of the variability in vaccine impact in our model was due to stochasticity, much was due to uncertainty in properties of the vaccine (Fig. 6C-F). With respect to cumulative infections averted in the 40 years following vaccine introduction, 50.6% of variation across the 2,500 simulation pairs was accounted for by a generalized additive model of cumulative infections averted as smooth functions of  $p$  and  $q$ . Dropping  $q$  as a predictor from the model led to a loss of only 0.1% of variation explained. Even so, smooth terms of  $p$  and  $q$  were both statistically significant in the combined model ( $p$ : effective d.f. = 6.7,  $F = 327.5$ ,  $P < 2 \times 10^{-16}$ ;  $q$ : e.d.f = 1.0,  $F = 6.7$ ,  $P < 0.01$ ). Similar effects were observed with respect to cumulative disease episodes averted in the 40 years following vaccine introduction ( $p$ : effective d.f. = 5.9,  $F = 189.1$ ,  $P < 2 \times 10^{-16}$ ;  $q$ : e.d.f = 1.0,  $F = 5.3$ ,  $P = 0.021$ ), although the proportion of variation in cumulative disease episodes averted that the model accounted for was less ( $R^2 = 0.35$ ).

For simulation pairs in which vaccine efficacy derived entirely from protection against disease rather than infection, there were zero infections averted over a 40-year time horizon on average (Fig. 6C). As the proportion of vaccine efficacy derived from protection against infection approached 20%, the proportion of infections averted over 40 years increased sharply but then increased more slowly for values of  $p$  in excess of 20% (Fig. 6C). In contrast, 28% of cumulative disease episodes 40 years after vaccine introduction were averted when vaccine efficacy derived entirely from protection against disease (Fig. 6D). When vaccine efficacy derived entirely from protection against infection, 79% of cumulative disease episodes 40 years after vaccine introduction were averted (Fig. 6D). Thus, the indirect effects associated with vaccination--i.e., preventing onward transmission from vaccine recipients--were 182% larger than the direct effects of vaccination in our model on a 40-year time horizon.

## DISCUSSION

We developed a new individual-based model for dengue transmission and applied it to questions regarding the impacts of uncertainty about different properties of the Dengvaxia® vaccine on projections of its public health impact. This analysis was not intended to represent a comprehensive assessment of the suitability of this vaccine as a public health tool or to make a recommendation about its use. Instead, the value of this analysis is that it provides a theoretical assessment of the extent to which different sources of uncertainty about the vaccine, of which there are many (27), might affect more detailed projections of public health impact that will inevitably follow. In summary, our results suggest that future projections of the vaccine's impact, applied either in specific settings or in generalities, should simulate across a range of multiple uncertainties about the vaccine's properties, particularly its mode of action. Limiting such projections to a specific set of assumptions about the vaccine's mode of action could result in the communication of recommendations to decision makers that convey a false sense of confidence.

Our results were unambiguous in their suggestion that the projected public health impact of Dengvaxia® is far more sensitive to biological uncertainty about the vaccine's mode of action than it is to statistical uncertainty about the numerical value of its efficacy against disease.

These results echo a previous analysis that highlighted fundamental problems that this type of biological uncertainty poses for estimates of the numerical value of efficacy against disease itself (9), which would effectively compound the biological uncertainty considered under our model. Between these two theoretical studies, it is clear that knowledge of both efficacy against disease and efficacy against infection would be extremely valuable. Even so, there are serious diagnostic limitations that impede the collection of the data that would be required to inform such estimates. There is extensive serological cross-reactivity of dengue and related viruses (35,36), and the same may also be true in the presence of vaccination. Similar challenges could plague the interpretation of Zika vaccine trial data, given that many Zika infections result in mild or asymptomatic infections (37) and may result in more severe disease among those with dengue antibodies (38).

The extent of differences that we observed due to biological uncertainty are a direct reflection of the extent of indirect effects of vaccination. Such effects have been predicted by models (39) and observed empirically (40) for a variety of diseases. One property that is expected to affect the extent of indirect effects is coverage (41), with high coverage potentially compensating somewhat for low efficacy. For Dengvaxia®, it is difficult to generalize about what coverage level might be appropriate or feasible in what setting. Another property that is expected to affect the extent of indirect effects are contact patterns (42). In our model, we quantified contact patterns in a more realistic way than other dengue transmission models by leveraging published, data-driven models pertaining to human movement (14) and human-mosquito contact (21) in Iquitos, Peru. Realistically modeling contact patterns, vaccine coverage, and other parameters of relevance to indirect effects are all important considerations for projections of public health impact, given the influence of indirect effects on cost-effectiveness calculations (43).

Although our model of vaccine efficacy is consistent with some findings from clinical trials of Dengvaxia® (6), such as serostatus- and age-dependent efficacy against disease, there are others that we have not accounted for. One notable feature of the vaccine is the appearance of possible serotype-specific efficacy, with low efficacy against disease resulting from serotype-2 infection being of greatest concern (44). A previous modeling analysis suggested that Dengvaxia® may have a net positive impact on public health despite this shortcoming (45). Other notable features of the vaccine that we have not considered pertain to protection against severe disease. In particular, to the extent that vaccination serves as a “primary-like” infection in seronegative vaccine recipients (27), the incidence of severe disease could increase as the proportion of seronegative vaccine recipients increases as transmission is lowered by indirect effects of vaccination (46). At the same time, clinical trial data suggest that whatever protection against severe disease the vaccine does afford wanes within a few years of vaccination (6). It will be important for modeling analyses that seek to inform policy recommendations to account for the full complexity of Dengvaxia®’s mode of action (47), but for the present analysis we chose to limit our assumptions about the vaccine to those that are most pertinent to our driving questions and that can be quantified using published data.

In addition to limitations associated with how we modeled Dengaxia's mode of action, there are a number of limitations of our transmission model. Perhaps most conspicuously, we did not account for seasonal transmission (11,48) and factors that give rise to it. Although we regard these details as nonessential for addressing our driving questions, accounting for seasonality will be a critical extension to the model if it is to be used for analyses that are intended to be directly relevant to specific locations and timeframes. We have also omitted a number of details about the ecology of *Aedes aegypti* mosquitoes, their encounters with humans, and how their contributions to transmission are affected by various types of vector control measures (2). Although such details may not be essential for analyses such as ours that focus solely on vaccines (49,50), they will be critical for realistic assessments of strategies that combine vaccination and vector control, which together offer the most promising strategy for abating the growing burden of dengue on global health (51).

## **ACKNOWLEDGEMENT**

This research made extensive use of computing resources provided by the Center for Research Computing at the University of Notre Dame.

## **FUNDING**

This research was supported by a grant from the US National Institutes of Health-National Institute of Allergy and Infectious Diseases (NIH/NIAID) award 1P01AI098670-01A1 (to TWS) and by the Research and Policy for Infectious Disease Dynamics (RAPIDD) program of the Science and Technology Directorate, Department of Homeland Security, and Fogarty International Center, National Institutes of Health. DLS was supported by a grant from the National Institutes of Health (ICMER U19 AI089674), and VAPS was supported by a grant from the NIH Fogarty International Center (K01TW008414-01A1). DLS and TAP were also supported by a grant from the Bill and Melinda Gates Foundation (OPP1110495), and TAP and QAT received support from the Eck Institute for Global Health.

## **COMPETING INTERESTS**

TAP, QAT, and GE receive partial support from a research contract from GlaxoSmithKline, which has a dengue vaccine candidate under development. GSK had no role in this study or in the preparation of this manuscript.

## **REFERENCES**

1. Gubler DJ. The economic burden of dengue. *Am J Trop Med Hyg.* 2012 May;86(5):743–4.
2. Achee NL, Gould F, Perkins TA, Reiner RC Jr, Morrison AC, Ritchie SA, et al. A critical assessment of vector control for dengue prevention. *PLoS Negl Trop Dis.* 2015 May;9(5):e0003655.
3. Morrison AC, Zielinski-Gutierrez E, Scott TW, Rosenberg R. Defining challenges and proposing solutions for control of the virus vector *Aedes aegypti*. *PLoS Med.* 2008 Mar

- 18;5(3):e68.
4. Vannice KS, Roehrig JT, Hombach J. Next generation dengue vaccines: A review of the preclinical development pipeline. *Vaccine*. 2015 Dec 10;33(50):7091–9.
  5. WHO | SAGE meeting of April 2016. World Health Organization; 2016 Apr 15 [cited 2016 Apr 30]; Available from: <http://www.who.int/immunization/sage/meetings/2016/april/en/>
  6. Hadinegoro SR, Arredondo-García JL, Capeding MR, Deseda C, Chotpitayasunondh T, Dietze R, et al. Efficacy and Long-Term Safety of a Dengue Vaccine in Regions of Endemic Disease. *N Engl J Med*. 2015 Sep 24;373(13):1195–206.
  7. Grange L, Simon-Loriere E, Sakuntabhai A, Gresh L, Paul R, Harris E. Epidemiological risk factors associated with high global frequency of inapparent dengue virus infections. *Front Immunol*. 2014 Jun 11;5:280.
  8. Duong V, Lambrechts L, Paul RE, Ly S, Lay RS, Long KC, et al. Asymptomatic humans transmit dengue virus to mosquitoes. *Proc Natl Acad Sci U S A*. 2015 Nov 24;112(47):14688–93.
  9. Rodriguez-Barraquer I, Mier-y-Teran-Romero L, Burke DS, Cummings DAT. Challenges in the Interpretation of Dengue Vaccine Trial Results. *PLoS Negl Trop Dis*. Public Library of Science; 2013 Aug 29;7(8):e2126.
  10. Morrison AC, Minnick SL, Rocha C, Forshey BM, Stoddard ST, Getis A, et al. Epidemiology of dengue virus in Iquitos, Peru 1999 to 2005: interepidemic and epidemic patterns of transmission. *PLoS Negl Trop Dis*. 2010 May 4;4(5):e670.
  11. Stoddard ST, Wearing HJ, Reiner RC Jr, Morrison AC, Astete H, Vilcarrromero S, et al. Long-term and seasonal dynamics of dengue in Iquitos, Peru. *PLoS Negl Trop Dis*. 2014 Jul;8(7):e3003.
  12. Chao DL, Halstead SB, Elizabeth Halloran M, Longini IM Jr. Controlling Dengue with Vaccines in Thailand. *PLoS Negl Trop Dis*. Public Library of Science; 2012 Oct 25;6(10):e1876.
  13. Karl S, Halder N, Kelso JK, Ritchie SA, Milne GJ. A spatial simulation model for dengue virus infection in urban areas. *BMC Infect Dis*. 2014 Aug 20;14:447.
  14. Perkins TA, Garcia AJ, Paz-Soldán VA, Stoddard ST, Reiner RC Jr, Vazquez-Prokopec G, et al. Theory and data for simulating fine-scale human movement in an urban environment. *J R Soc Interface* [Internet]. 2014 Oct 6;11(99). Available from: <http://dx.doi.org/10.1098/rsif.2014.0642>
  15. Getis A, Morrison AC, Gray K, Scott TW. Characteristics of the spatial pattern of the dengue vector, *Aedes aegypti*, in Iquitos, Peru. *Am J Trop Med Hyg*. 2003 Nov;69(5):494–505.
  16. Grimm V, Berger U, Bastiansen F, Eliassen S, Ginot V, Giske J, et al. A standard protocol for describing individual-based and agent-based models. *Ecol Modell*. 2006 Sep 15;198(1–2):115–26.
  17. Grimm V, Berger U, DeAngelis DL, Polhill JG, Giske J, Railsback SF. The ODD protocol: A

- review and first update. *Ecol Modell.* 2010 Nov 24;221(23):2760–8.
18. Prothero RM. Disease and mobility: a neglected factor in epidemiology. *Int J Epidemiol.* 1977 Sep;6(3):259–67.
  19. Harrington LC, Scott TW, Lerdthusnee K, Coleman RC, Costero A, Clark GG, et al. Dispersal of the dengue vector *Aedes aegypti* within and between rural communities. *Am J Trop Med Hyg.* 2005 Feb;72(2):209–20.
  20. Scott TW, Amerasinghe PH, Morrison AC, Lorenz LH, Clark GG, Strickman D, et al. Longitudinal studies of *Aedes aegypti* (Diptera: Culicidae) in Thailand and Puerto Rico: blood feeding frequency. *J Med Entomol.* 2000 Jan;37(1):89–101.
  21. Liebman KA, Stoddard ST, Reiner RC Jr, Perkins TA, Astete H, Sihuincha M, et al. Determinants of heterogeneous blood feeding patterns by *Aedes aegypti* in Iquitos, Peru. *PLoS Negl Trop Dis.* 2014 Feb;8(2):e2702.
  22. Nguyen NM, Thi Hue Kien D, Tuan TV, Quyen NTH, Tran CNB, Vo Thi L, et al. Host and viral features of human dengue cases shape the population of infected and infectious *Aedes aegypti* mosquitoes. *Proceedings of the National Academy of Sciences.* 2013 May 28;110(22):9072–7.
  23. Chan M, Johansson MA. The incubation periods of Dengue viruses. *PLoS One.* 2012 Nov 30;7(11):e50972.
  24. Simmons CP. A Candidate Dengue Vaccine Walks a Tightrope. *N Engl J Med.* 2015 Sep 24;373(13):1263–4.
  25. Guagliardo SA, Morrison AC, Barboza JL, Requena E, Astete H, Vazquez-Prokopec G, et al. River boats contribute to the regional spread of the dengue vector *Aedes aegypti* in the Peruvian Amazon. *PLoS Negl Trop Dis.* 2015 Apr;9(4):e0003648.
  26. Reich NG, Shrestha S, King AA, Rohani P, Lessler J, Kalayanarooj S, et al. Interactions between serotypes of dengue highlight epidemiological impact of cross-immunity. *J R Soc Interface.* 2013 Sep 6;10(86):20130414.
  27. Guy B, Jackson N. Dengue vaccine: hypotheses to understand CYD-TDV-induced protection. *Nat Rev Microbiol.* 2016 Jan;14(1):45–54.
  28. Team RC. R: A language and environment for statistical computing. R Foundation for Statistical Computing, Vienna, Austria. 2013. ISBN 3-900051-07-0; 2014.
  29. Ewell M. Comparing methods for calculating confidence intervals for vaccine efficacy. *Stat Med.* 1996;15(21-22):2379–92.
  30. Statistical Inference for Partially Observed Markov Processes [R package pomp version 1.4.1.1]. Comprehensive R Archive Network (CRAN); [cited 2016 May 1]; Available from: <https://cran.r-project.org/web/packages/pomp/index.html>
  31. Anderson RM, May RM, Anderson B. Infectious diseases of humans: dynamics and control. Vol. 28. Wiley Online Library; 1992.
  32. Ellis AM, Garcia AJ, Focks DA, Morrison AC, Scott TW. Parameterization and sensitivity

- analysis of a complex simulation model for mosquito population dynamics, dengue transmission, and their control. *Am J Trop Med Hyg.* ASTMH; 2011 Aug;85(2):257–64.
33. Magori K, Legros M, Puente ME, Focks DA, Scott TW, Lloyd AL, et al. Skeeter Buster: a stochastic, spatially explicit modeling tool for studying *Aedes aegypti* population replacement and population suppression strategies. *PLoS Negl Trop Dis.* 2009 Sep 1;3(9):e508.
  34. Wood S. Generalized additive models: an introduction with R. CRC press; 2006.
  35. Innis BL, Nisalak A, Nimmannitya S, Kusalerdchariya S, Chongswasdi V, Suntayakorn S, et al. An enzyme-linked immunosorbent assay to characterize dengue infections where dengue and Japanese encephalitis co-circulate. *Am J Trop Med Hyg.* 1989 Apr;40(4):418–27.
  36. Tang KF, Ooi EE. Diagnosis of dengue: an update. *Expert Rev Anti Infect Ther.* 2012 Aug;10(8):895–907.
  37. Duffy MR, Chen T-H, Hancock WT, Powers AM, Kool JL, Lanciotti RS, et al. Zika virus outbreak on Yap Island, Federated States of Micronesia. *N Engl J Med.* 2009 Jun 11;360(24):2536–43.
  38. Paul LM, Carlin ER, Jenkins MM, Tan AL, Barcellona CM, Nicholson CO, et al. Dengue Virus Antibodies Enhance Zika Virus Infection [Internet]. *bioRxiv.* 2016 [cited 2016 Apr 30]. p. 050112. Available from: <http://biorxiv.org/content/early/2016/04/25/050112>
  39. Van Effelterre T, Soriano-Gabarró M, Debrus S, Claire Newbern E, Gray J. A mathematical model of the indirect effects of rotavirus vaccination. *Epidemiol Infect.* 2010 Jun;138(6):884–97.
  40. Jordan R, Connock M, Albon E, Fry-Smith A, Olowokure B, Hawker J, et al. Universal vaccination of children against influenza: are there indirect benefits to the community? A systematic review of the evidence. *Vaccine.* 2006 Feb 20;24(8):1047–62.
  41. Garnett GP. Role of herd immunity in determining the effect of vaccines against sexually transmitted disease. *J Infect Dis.* 2005 Feb 1;191 Suppl 1:S97–106.
  42. Ma J, van den Driessche P, Willeboordse FH. The importance of contact network topology for the success of vaccination strategies. *J Theor Biol.* 2013 May 21;325:12–21.
  43. Brisson M, Edmunds WJ. Impact of model, methodological, and parameter uncertainty in the economic analysis of vaccination programs. *Med Decis Making.* 2006 Sep;26(5):434–46.
  44. Sabchareon A, Wallace D, Sirivichayakul C, Limkittikul K, Chanthavanich P, Suvannadabba S, et al. Protective efficacy of the recombinant, live-attenuated, CYD tetravalent dengue vaccine in Thai schoolchildren: a randomised, controlled phase 2b trial. *Lancet.* 2012 Nov 3;380(9853):1559–67.
  45. Rodriguez-Barraquer I, Mier-y-Teran-Romero L, Schwartz IB, Burke DS, Cummings DAT. Potential opportunities and perils of imperfect dengue vaccines. *Vaccine.* Elsevier; 2014 Jan 16;32(4):514–20.

46. Rodriguez-Barraquer I, Mier-y-Teran-Romero L, Ferguson N, Burke DS, Cummings DAT. Differential efficacy of dengue vaccine by immune status. *Lancet*. 2015 May 2;385(9979):1726.
47. Saadatian-Elahi M, Horstick O, Breiman RF, Gessner BD, Gubler DJ, Louis J, et al. Beyond efficacy: The full public health impact of vaccines. *Vaccine*. 2016 Feb 24;34(9):1139–47.
48. Reiner RC Jr, Stoddard ST, Forshey BM, King AA, Ellis AM, Lloyd AL, et al. Time-varying, serotype-specific force of infection of dengue virus. *Proc Natl Acad Sci U S A*. 2014 Jul 1;111(26):E2694–702.
49. Chao DL, Longini IM Jr, Halloran ME. The effects of vector movement and distribution in a mathematical model of dengue transmission. *PLoS One*. 2013 Oct 21;8(10):e76044.
50. Pandey A, Mubayi A, Medlock J. Comparing vector–host and SIR models for dengue transmission. *Math Biosci*. 2013 Dec;246(2):252–9.
51. Gubler DJ. The partnership for dengue control - a new global alliance for the prevention and control of dengue. *Vaccine*. 2015 Mar 3;33(10):1233.
52. Gillespie DT. Exact stochastic simulation of coupled chemical reactions. *J Phys Chem*. 1977;81(25):2340–61.
53. Glass K, Xia Y, Grenfell BT. Interpreting time-series analyses for continuous-time biological models—measles as a case study. *J Theor Biol*. 2003 Jul 7;223(1):19–25.
54. Sabin AB. Research on dengue during World War II. *Am J Trop Med Hyg*. 1952 Jan;1(1):30–50.
55. UNdata [Internet]. [cited 2016 Apr 30]. Available from: <http://data.un.org>
56. Olkowski S, Forshey BM, Morrison AC, Rocha C, Vilcarrero S, Halsey ES, et al. Reduced risk of disease during post-secondary dengue virus infections. *J Infect Dis* [Internet]. 2013 Jun 17; Available from: <http://jid.oxfordjournals.org/content/early/2013/06/16/infdis.jit273.abstract>
57. Nishiura H, Halstead SB. Natural History of Dengue Virus (DENV)—1 and DENV—4 Infections: Reanalysis of Classic Studies. *J Infect Dis* [Internet]. [jid.oxfordjournals.org](http://jid.oxfordjournals.org); 2007; Available from: <https://jid.oxfordjournals.org/content/195/7/1007.full>
58. Penny MA, Verity R, Bever CA, Sauboin C, Galaktionova K, Flasche S, et al. Public health impact and cost-effectiveness of the RTS,S/AS01 malaria vaccine: a systematic comparison of predictions from four mathematical models. *Lancet*. 387(10016):367–75.

## TABLE

**Table 1.** Definitions of key terms.

Term	Symbol	Definition
Relative risk of disease conditional on infection	$RR_{dis inf}$	Proportion of vaccine recipients that experience disease after becoming infected relative to the proportion of placebo recipients that experience disease after becoming infected.
Relative risk of infection conditional on exposure	$RR_{inf exp}$	Proportion of vaccine recipients that become infected after being bitten by an infectious mosquito relative to the proportion of placebo recipients that become infected after being bitten by an infectious mosquito.
Relative risk of disease	$RR_{dis}$	Proportion of vaccine recipients that experience disease after being bitten by an infectious mosquito relative to the proportion of placebo recipients that experience disease after being bitten by an infectious mosquito. This is equal to the product of $RR_{dis inf}$ and $RR_{inf exp}$ .
Vaccine efficacy against disease	$VE_{dis}$	$1 - RR_{dis}$
Proportion of protection against disease derived from protection against infection	$p$	This parameter relates $RR_{inf exp}$ to $RR_{dis}$ according to the relationship $RR_{inf exp} = RR_{dis}^p$ . Likewise, it is implied that $RR_{dis inf} = RR_{dis}^{1-p}$ and $RR_{dis} = RR_{dis inf} \times RR_{inf exp}$ .
Quantile of $RR_{dis}$ estimate	$q$	Quantile between 0 and 1 applied to the uncertainty distribution of the $RR_{dis}$ estimate.

## FIGURES

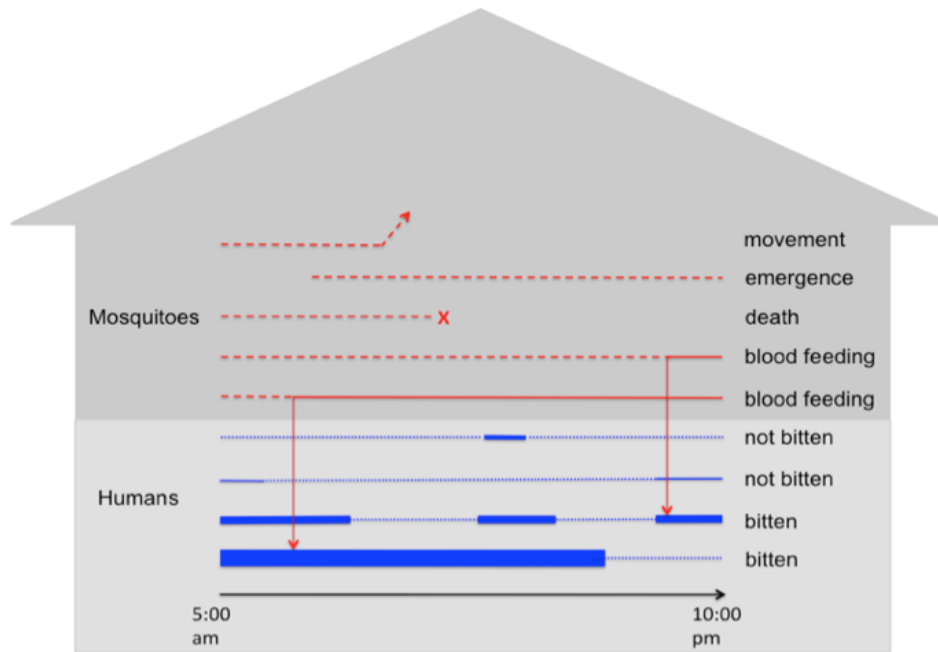


**Figure 1.** Example of events that occur over the course of a single day at a single location. Red lines correspond to individual mosquitoes, with dashed and solid lines representing blood-feeding and resting states, respectively. Blue lines refer to individual people, with thin dotted lines indicating that the person is at another location at that time and thick solid lines indicating their presence at the location at that time. The thickness of the solid blue lines indicates the relative attractiveness of each person to blood feeding by mosquitoes.

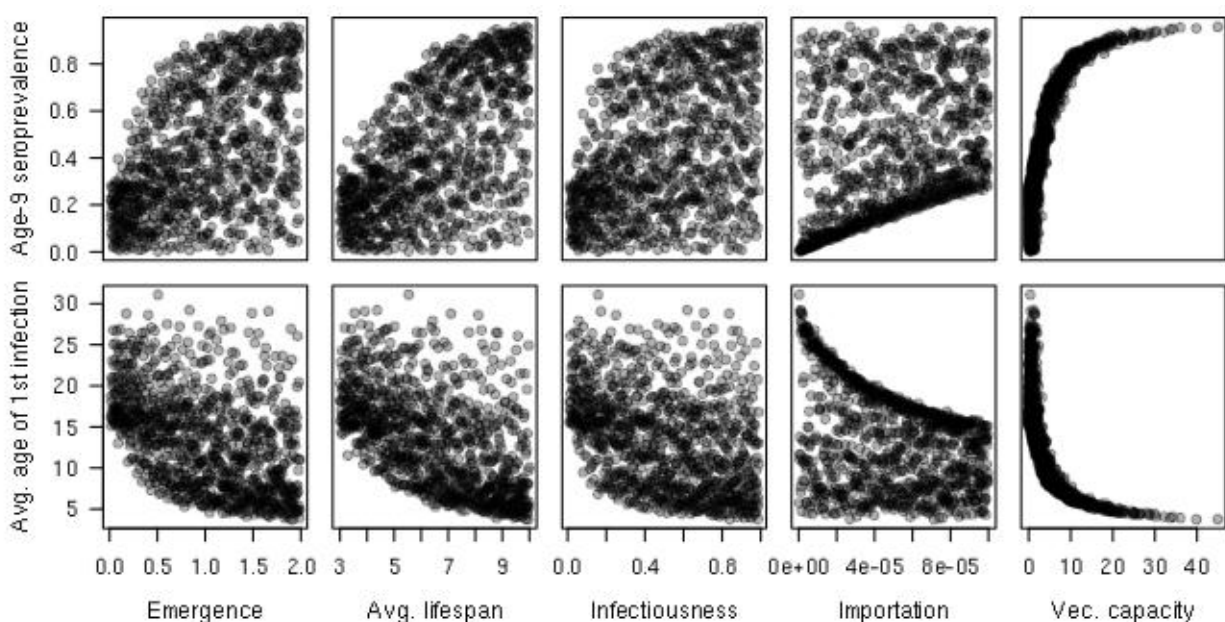


**Figure 2.** Relationships between free parameters in the model (emergence, average adult mosquito lifespan, mosquito infectiousness, force of infection due to importation), vectorial capacity (which depends on the first three parameters), and two epidemiological metrics (age-9 seroprevalence, average age of first infection). Each point represents the value of the metric after 40 simulated years of transmission in a single realization of the model with no vaccination.

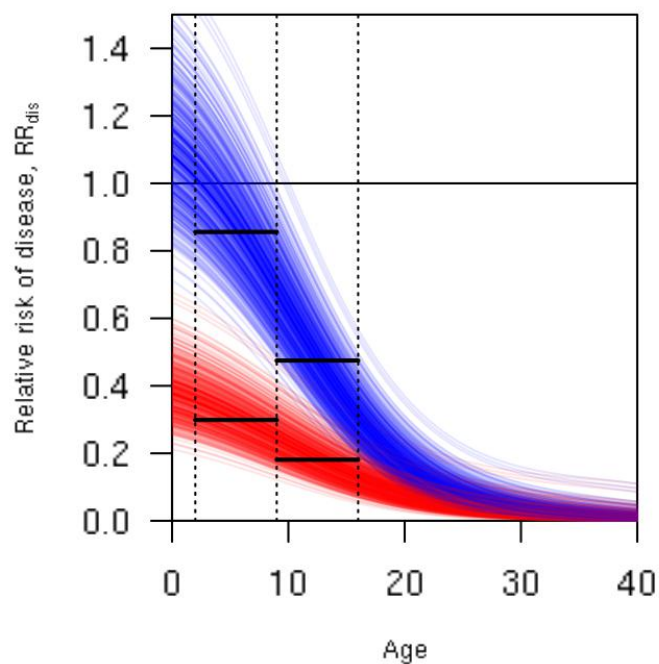


**Figure 3.** Relative risk of disease,  $RR_{dis}$ , as a function of age and serostatus (blue = seronegative, red = seropositive) estimated from vaccine trial data (6). Each line represents a distinct random draw. Horizontal bars correspond to estimates of relative risk of disease in the trial for a given age group (2-9, 9-16) and serostatus.

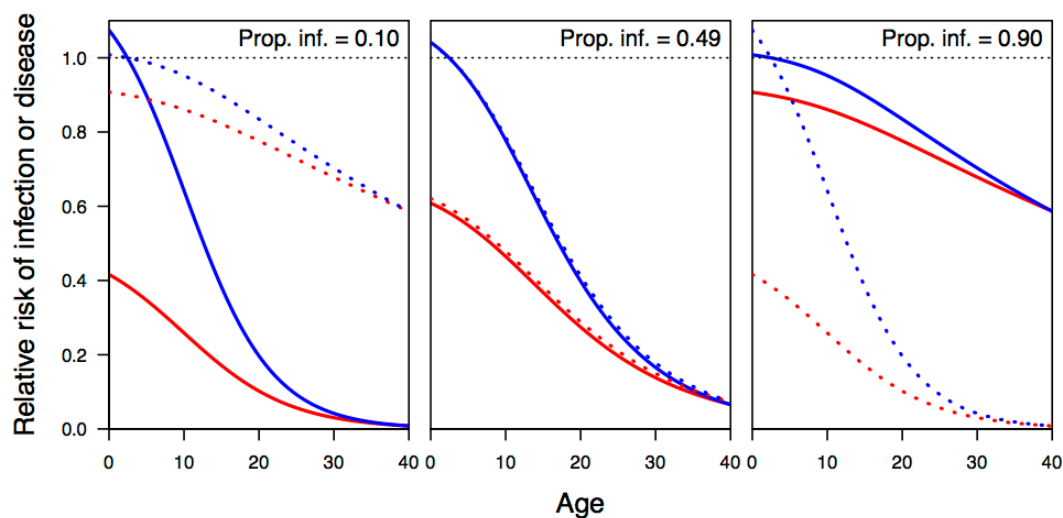


**Figure 4.** Relative risk of infection conditional on exposure (dashed) and of disease conditional on infection (solid) for seropositive (red) and seronegative (blue) individuals of different ages. These relationships are shown for three different values of the parameter  $p$  that specifies the proportion of the overall efficacy against disease that is attributable to protection against infection conditional on exposure.

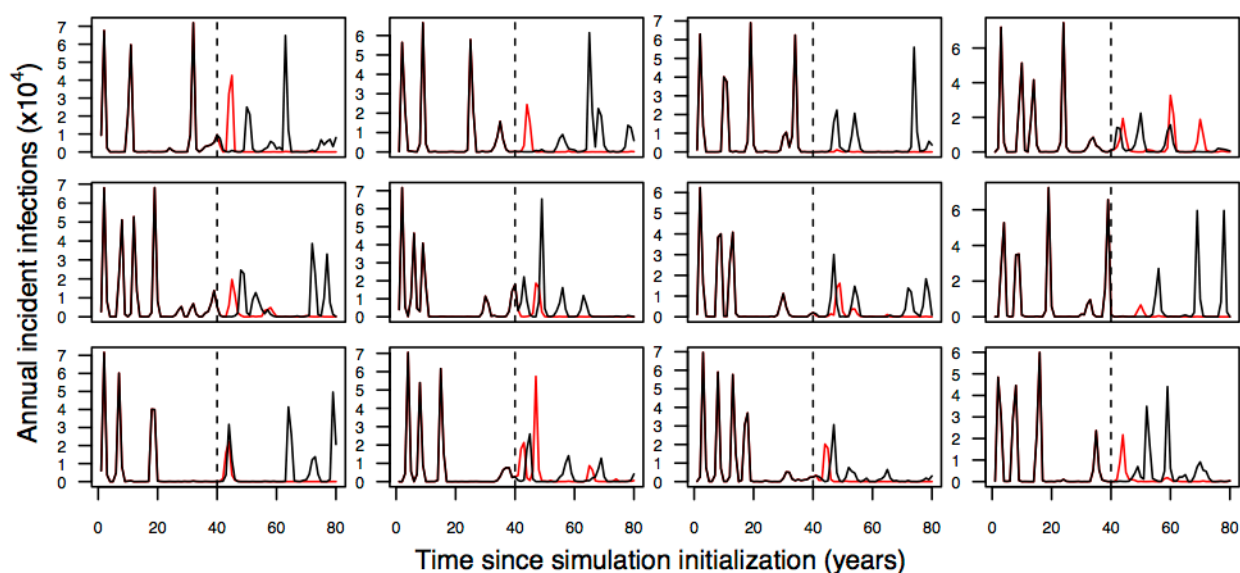


**Figure 5.** Example time series of annual incident infections simulated from the model. Each panel shows a pair of simulations with two common random number streams for (i) events related to the demography, movement, and mixing of mosquitoes and people, and (ii) events related to infection and disease. Each pair of simulations differs beginning in year 40, when routine vaccination commences in the simulation colored in red but not in the one in black.

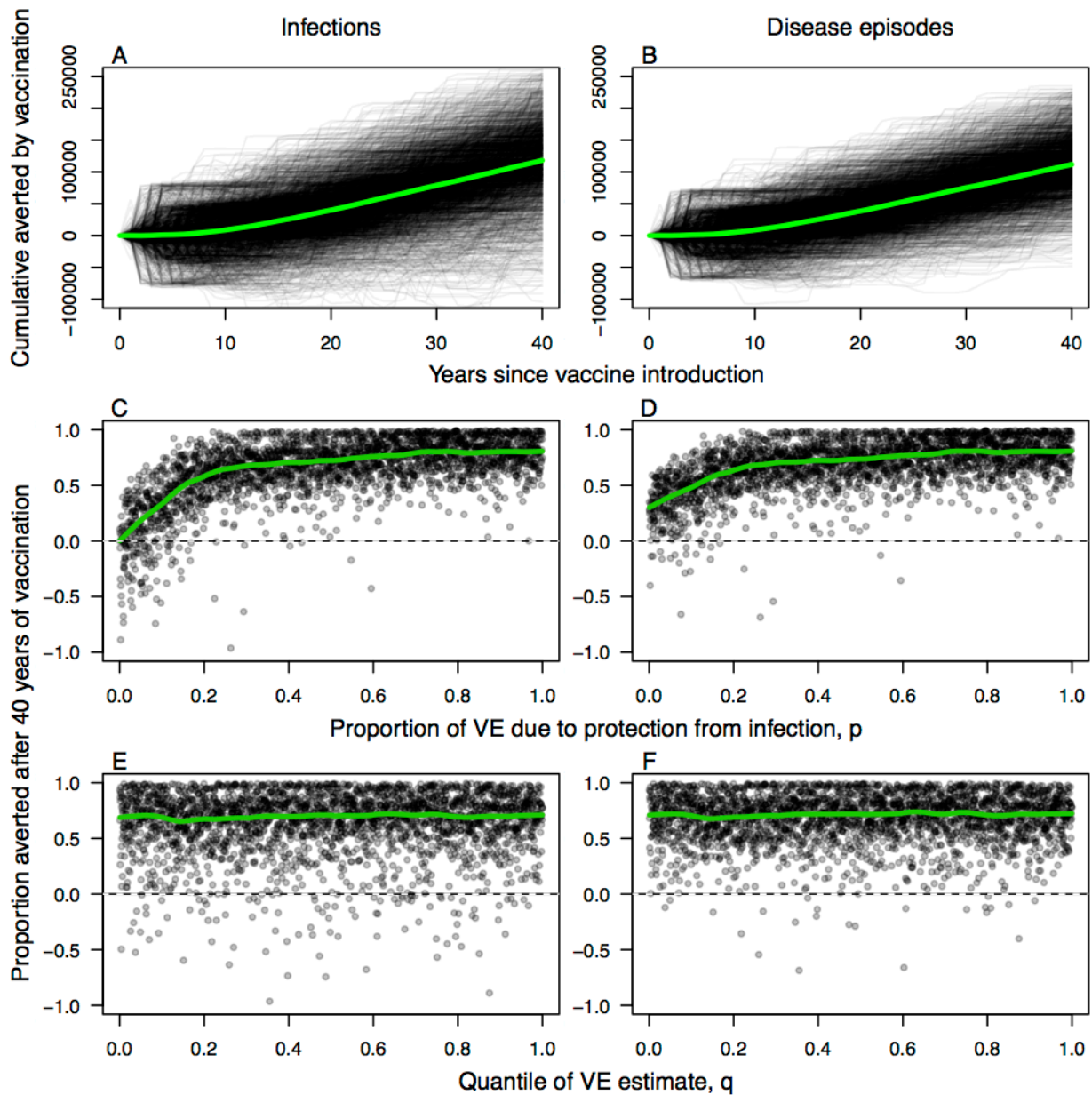


**Figure 6.** Impacts of vaccination assessed in 2,500 pairs of simulations with and without vaccination, with simulation pairs varying with respect to the proportion of vaccine efficacy due to protection from infection,  $p$ , and the quantile of estimated vaccine efficacy,  $q$ . Infections and disease episodes averted were calculated as the number in the simulation without vaccination minus the number in the simulation with vaccination. Cumulative numbers averted in each year since vaccination 1-40 are shown in A & B, and the proportion averted after 40 years of vaccination are shown in C & D as a function of  $p$  and in E & F as a function of  $q$ . Green lines in A & B are averages in each year and in C-F are loess regressions intended to show running averages.

## SUPPORTING INFORMATION

### Detailed Model Description

This model description follows the ODD (Overview, Design concepts, Details) protocol for individual-based models (16,17). Given how complex individual-based models can be, the ODD protocol was developed as a way to standardize the description of these models throughout ecology and other fields. This model has been implemented as a software program using object-oriented code in C++.

#### Purpose

The model simulates transmission of dengue viruses between individual people and mosquitoes that occupy a landscape of discrete locations where they encounter each other. The model also simulates the impact of a dengue vaccine on the occurrence of dengue virus infection, mild disease associated with DENV infection, and severe disease associated with DENV infection within the simulated human population.

#### Entities, state variables, and scales

The model focuses on five primary entities: individual people, individual mosquitoes, infections, locations, and vaccines. Individual people have the following state variables: a location that is designated as the individual's home, an activity space, gender, body size, infection status, infection history, and immune status. Individual mosquitoes have the following state variables: location and infection status. All individual mosquitoes are adult female *Aedes aegypti*. Infections have the following state variables: dengue serotype 1-4, day of infection, and, for infections in humans, day of recovery and immune acquisition. Locations have the following state variables: longitudinal and latitudinal coordinates of the location's centroid, location type (residential, commercial, recreation, education, health care, religion, institutions, others), and daily emergence rates of newly eclosed mosquitoes. Vaccines have the following two state variables: efficacy against disease as a function of the age and pre-exposure history of the vaccinee, and the proportion of that efficacy attributable to protection against disease conditional on infection versus protection against infection conditional on exposure. Each of these five entities is defined by its own object class in our code.

For purposes of software implementation, our model is, on one level, iterated on a daily basis. On another level and for most processes, however, our model treats time in a continuous fashion because it is fundamentally an event-based model, analogous to the Gillespie algorithm (52). We made this decision to minimize inaccuracies associated with lumping and discretizing events that occur continuously (53), to avoid being forced to make a fixed decision about the order of different types of events, and to allow for maximal precision in describing probabilistic distributions of waiting times for various stochastic processes. This precision is important not only for realistic modeling of the temporal dynamics of transmission but will be increasingly important in the future to realistically account for the sometimes subtle effects that mosquito-based interventions can have; e.g., reducing mosquito biting rates. The fundamental spatial unit

in the model is the location, which we model after a city lot that each house or other building sits on. Altogether, our model applies to 40,839 lots, comprised primarily of homes but also including shops, markets, schools, churches, parks, and other locations. This constitutes the entirety of the core of the city of Iquitos, where the majority of relevant data collection has occurred over the last 15+ years and where roughly half of the entire metropolitan population lives.

### Process overview and scheduling

The key processes in the model are 1) movement by individual people, 2) movement by mosquitoes, 3) mosquito emergence, 4) mosquito death, 5) mosquito blood-feeding, 6) infection of susceptible people by infectious mosquitoes or 7) vice versa, 8) changes in the infectiousness of individual people over time, 9) changes in the immune status of individual people, 10) demographic changes in the human population, and 11) vaccination. The first of these processes is pre-calculated and incorporated into the model as an input. The timing until an event of each of the other types occurs is represented as a continuous random variable, such that events occur at specific times of day. These random variables are drawn from probability distributions described separately for each process in the Submodels section. An illustration of the continuous timing of events related to mosquito-host encounters is shown in Fig. 1.

On a daily basis, the model iterates through each mosquito in the city and executes the events scheduled for that mosquito for that day in the order in which the events are scheduled to occur. One example of why this scheduling is important is if a mosquito is scheduled to both die and infect someone in the same day, the infection will never occur if death takes place first. Because events that apply to one mosquito have no effect on any other mosquitoes on that day, the order in which individual mosquitoes are processed is inconsequential. Mosquitoes are also assumed to have no effect on a human's status within a day, and instead rely only on each person's pre-scheduled whereabouts when selecting a person upon whom to blood-feed. This decoupling of event scheduling within versus across days is possible because the onset of infectiousness in both people and mosquitoes always takes longer than a single day (23,54).

### Design concepts

#### *Basic principles*

The model seeks to leverage years of studies in Iquitos, Peru, quantifying heterogeneities in DENV transmission that manifest at individual, household, and neighborhood scales. Priorities for the model include realistically modeling individual human movement patterns and biting heterogeneity among individuals simultaneously co-located at a single location. We also seek to model details of infection dynamics and vaccine effects at an individual level in accordance with the best available data from clinical trials.

#### *Emergence*

Patterns of DENV infection in space and time are emergent properties of the model and are not predefined. Stochasticity is the major driver of a priori uncertainty about these patterns.

### *Adaptation*

The mosquito's decision about whom to bite is influenced by the number of people present at a given time and each person's attractiveness to mosquitoes (21).

### *Objectives*

The only entities in the model with any explicit objectives are mosquitoes, which seek to blood-feed. That said, they suffer no penalty nor reap any reward as a consequence of failing or succeeding in their quest to blood-feed.

### *Learning*

None of the entities in the model have a learning capacity.

### *Prediction*

None of the entities in the model have a predictive capacity.

### *Sensing*

Each mosquito has the ability to sense the number of people present at its current location at a given time of day, as well as the attractiveness for blood-feeding on each person. The latter is a human state variable that depends on body surface area (21). No mosquito is able to sense the presence or attractiveness of people at locations at which the mosquito is not currently present. As a consequence, their movement decisions are not affected by the presence or attractiveness of people at a location to which they might move.

### *Interaction*

Mosquitoes interact with humans through blood-feeding and through the associated transmission of viruses in some cases. The movement trajectories of people are not affected by having been blood-fed upon.

### *Stochasticity*

Prior to being incorporated into the model as an input, human movement trajectories are generated from a continuous-time Markov chain according to the algorithm by Perkins et al. (14). Practically, this means that the duration of a visit to a given location is drawn from an exponential distribution and that the next location an individual visits is drawn from a categorical distribution over all other locations in an individual's activity space. The rates of these exponential distributions are related to the duration of visits to each location, and the probabilities of the categorical distributions are related to the frequency of visits to each location. Proceeding each day after initialization, one of the individual's daily trajectories is selected with equal probability.

Mosquito lifespan is drawn from an exponential distribution at the time of a mosquito's emergence. Mosquito movement is also highly stochastic, with the decision to stay or leave a location on a given day determined by a Bernoulli trial and the mosquito's destination location

drawn randomly from the set of all locations within 50 meters with even probability. The elapsed time before a mosquito blood-feeds again is drawn from an exponential.

A mosquito blood-feeds on a person at its current location, with the identity of that person determined by a random draw from a categorical distribution with probabilities proportional to each person's biting attractiveness (21). If either a mosquito is infectious and a person susceptible or vice versa, an infection results depending on the outcome of a Bernoulli trial. Thenceforth, the duration of the incubation period in a given mosquito is drawn randomly from a predefined lognormal distribution specified based on empirical studies (23). Lastly, the duration of temporary cross-immunity in a given person is drawn randomly from an exponential distribution (26).

For the sake of comparability across analyses, we use two distinct random number seeds in each simulation. One applies to events that directly involve vaccines or viruses, whereas the other applies to other events, most of which have to do with demographic events, movement, and human-mosquito contact. This allows for the landscape of human-mosquito encounters to unfold identically across multiple simulations in which aspects of vaccination can be varied separately.

### *Collectives*

Each person is assigned to a home location and as such is part of a household. Membership in a household comes with no special properties in the model other than the general tendency to spend more time at that common location than they would otherwise. Altogether, we considered a population of 200,000 people living in 38,835 houses within a total landscape of 40,839 locations.

### *Observation*

The model is capable of producing a variety of different output files that report infections and other events, either individually or aggregated temporally and/or spatially.

### Initialization

The composition of each house (i.e., how many residents plus each person's age, sex, and body size) was obtained by simulating a population with house-level demographic profiles consistent with available survey data but conforming to a desired total population size and age and gender distribution (55).

The first step in the population simulation algorithm was to simulate household sizes that yielded the correct overall population size. To do so, we weighted the distribution of household sizes in the survey data by a geometric probability mass function with a fitted parameter  $p=0.34$ . Sampling 38,835 houses weighted in this way yielded an appropriately sized overall population of 200,000 individuals on average. The second step in the population simulation algorithm was to randomly draw demographic profiles for houses of each size from the survey data. We populated houses serially, keeping track of the number of simulated individuals of each age and gender as the simulation proceeded. Once a given age-gender combination was exhausted in

the target age and gender distribution, we attempted to replace the individual in question with one of the same gender and age class (i.e., children under 18, adults 18+). Near the end of the population simulation routine, however, we deviated from the target age class and/or gender of the simulated individual in question. For example, this resulted in some of the very last simulated houses being inhabited by several adult men, which was a household profile not observed in the survey data but one that was necessary to obtain a realistic age and gender distribution for the population as a whole.

Once the initial population was simulated, we simulated each person's serostatus for each of the four DENV serotypes as a function of that person's age and a free parameter describing a baseline force of infection due to infections acquired when visiting areas outside Iquitos, which we refer to as "force of importation." No infections due to transmission within Iquitos were accounted for at the time of initialization. Instead, a burn-in period of 40 years was simulated to allow for acquisition of locally acquired infections prior to vaccination.

The number of mosquitoes that emerge in each location on each day of the simulation is simulated as a Poisson random variable with rate determined by a free parameter. The model was initialized with no infected or infectious mosquitoes.

### Input

Each realization of the model depends on inputs from three files. There is a single master file in which each row specifies input files and values of parameters that vary across realizations of the model. The first of the primary input files contains rows that each describes a location and its attributes. A second file contains five sample daily movement trajectories for each individual, as well as their personal attributes. A third file contains parameters that describe the vaccine's efficacy as a function of vaccinee age and pre-exposure history, as well as values of the model's free parameters.

### Submodels

#### *Movement by individual people*

We adopt a submodel for movement by people described by Perkins et al. (14). This model offers a means to simulate an individual's activity space, which is defined as both the collection of locations that a person visits as a matter of routine and a description of the proportion of time the person spends at each of those locations. The model furthermore specifies that a person moves about those locations through time according to a continuous-time Markov process, which depends on simulated values of two key attributes of a person's connection to a location: how often they visit the location and how long they stay there during each visit, on average.

This submodel was fitted to data from retrospective, semi-structured interviews of residents of Iquitos. These interviews were structured in such a way as to facilitate recall of specific locations visited during specific timeframes during the two weeks preceding the interview. Fitting this model to those data, Perkins et al. (14) found that location type and distance from home significantly affect a person's likelihood of visiting a location and also how often and for how long they visit. Furthermore, by accounting for the availability of locations at different distances

from home depending on where a person lives (e.g., in the city center or on the periphery), the model successfully accounted for differences in movement patterns of residents living in two different neighborhoods in Iquitos. This finding is significant because it suggests that this submodel can be reasonably applied to simulated residents throughout the city and not just within the study area. The fitted movement model is also representative in the sense that interviews were conducted on a diverse group of individuals of different ages, sexes, and occupations (14).

For application to the model, we use this submodel to simulate five stochastic realizations of a daily movement trajectory for each simulated person in our synthetic population. Each trajectory consists of a sequence of locations and what fraction of the day is spent at each location during each visit. These movement trajectories are incorporated into the model through an input file. At the beginning of each simulated day, one of these trajectories is randomly chosen and followed for that day.

#### *Movement by mosquitoes*

Each mosquito has a constant probability of 70% of staying at its current location for a given day (19). If it moves, the location to which it moves is drawn randomly from all locations within a 50 meter radius of the mosquito's location.

#### *Mosquito emergence*

Daily emergence of mosquitoes at each location occurs according to a Poisson random draw with rate equal to a free parameter. This rate does not vary in space or time, which means that, on average, the number of mosquitoes at each location is equal to the emergence rate multiplied by average mosquito lifespan.

#### *Mosquito death*

We assume that mosquitoes experience death at a constant rate and do not senesce. We implement this by assigning each mosquito with an adult lifespan at its time of emergence, drawing this number from an exponential distribution with rate determined by a free parameter.

#### *Mosquito blood-feeding*

Upon emergence, a mosquito refrains from attempting to bite for an exponentially distributed period of time, with the average duration of that period set to 1.5 days (20). The mosquito selects a particular person on whom to blood-feed by taking a random draw from a categorical distribution informed by a function of the body size of all people present at the location at that time (21). If no people are present, the mosquito is assumed to either find another source of blood or wait until its next scheduled blood meal, which is also exponentially distributed with average duration of 1.5 days (20).

#### *Infection of susceptible people by infectious mosquitoes*

After a bite by an infectious mosquito, a susceptible human becomes infected with a probability determined by a free parameter. Infections develop symptomatic disease with probabilities dependent on the number of previous exposures to dengue that they have experienced: 23.5%

for those with no previous exposures, 16% for those with one previous exposure, and 4% for those with two or three previous exposures (56).

#### *Infection of susceptible mosquitoes by infectious people*

When blood-feeding on an infectious person, a susceptible mosquito is infected with a probability determined by the person's infectiousness. A person's infectiousness on a given day since infection was derived from an analysis by Nishiura and Halstead (57) of data on human infectiousness originally published by Sabin (54). We approximated the infectiousness data as presented by Nishiura and Halstead with the function

$$1.01 e^{-0.278 (t - (IIP - 0.288))^2},$$

where  $t$  is the number of days since the human was infected by a mosquito and  $IIP$  is the length of the incubation period in the human (intrinsic incubation period). Each person is assigned an  $IIP$  by taking a random draw from a lognormal distribution fitted by Chan and Johansson (23). To model whether successful infection occurred, a Bernoulli trial is performed with a probability of infection equal to that person's infectiousness on that day. Upon infection, mosquitoes enter a period of latent infection for a period of time drawn from an empirically estimated lognormal distribution with a mean of 6.5 days parameterized at a constant temperature of 30 °C (23). Upon completion of the latent period, a mosquito becomes infectious and remains so for the remainder of its life. If a mosquito is exposed subsequent to becoming infected, the latter exposure has no impact on the outcome of the initial infection (e.g., an individual mosquito can only ever be infected by a single virus serotype).

#### *Changes in the immune status of individual people*

Following infection with dengue viruses, it is generally accepted that there is a temporary period of heterologous immunity. We implement a published model (26) whereby individuals are completely protected following an infection, but the duration of this protection for each individual is drawn independently from an exponential distribution with a mean of 686 days. At the conclusion of the individual's period of heterologous immunity, they resume their susceptibility to serotypes to which they have no prior exposure.

#### *Demographic changes in the human population*

We maintain a stable human population age structure representative of Peru (55) by applying a linearly increasing age-dependent death rate of  $6.9 \times 10^{-9}$  times a person's age in days and replacing each newly deceased person with a newborn child. Children are born with a normally distributed body surface area that grows linearly to a normally distributed adult body surface area that is attained at a threshold age. We fitted sex-specific parameters for these parameters using biometric data collected during a study of heterogeneous biting in Iquitos (21). These parameters include body size at birth for males  $\sim N(0.31, 0.30)$  and females  $\sim N(0.31, 0.18)$ , final adult body sizes for males  $\sim N(1.71, 0.30)$  and females  $\sim N(1.51, 0.24)$ , and the ages at which adult body sizes were attained for males = 18.65 and females = 16.52. These parameters were sufficient to linearly interpolate body sizes between birth and adulthood.

### *Vaccination*

We distribute a vaccine resembling the Dengvaxia® vaccine to 90% of children on their ninth birthday, and we assume that 100% of vaccinees comply with the full vaccination schedule of three doses over 12 months. We assume 90% initial compliance and 100% follow-up compliance in accordance with previous modeling assessments of vaccine impact (58), and we apply the vaccine at age 9 consistent with current recommendations for this vaccine (5). We assume that the efficacy of the vaccine tracks the relationship in eqn. (1) as an individual ages and in the event of a change in serostatus from negative to positive. To specify the portion of overall efficacy in  $VE_{dis}$  that derives from protection against infection versus protection against disease conditional on infection, we used a free parameter  $p$  to specify the relative reduction in infection as  $(1 - VE_{dis})^p$  and relative reduction in disease conditional on infection as  $(1 - VE_{dis})^{1-p}$  (Fig. 4).